Nuclear mRNA export requires specific FG nucleoporins for translocation through the nuclear pore complex

Laura J. Terry and Susan R. Wente

Department of Cell and Developmental Biology, Vanderbilt University Medical Center, Nashville, TN 37232

Trafficking of nucleic acids and large proteins through nuclear pore complexes (NPCs) requires interactions with NPC proteins that harbor FG (phenylalanine-glycine) repeat domains. Specialized transport receptors that recognize cargo and bind FG domains facilitate these interactions. Whether different transport receptors utilize preferential FG domains in intact NPCs is not fully resolved. In this study, we use a large-scale deletion strategy in *Saccharomyces cerevisiae* to generate a new set of *more minimal pore* (*mmp*) mutants that lack specific FG domains. A comparison of messenger RNA (mRNA) export versus protein import reveals unique subsets of *mmp* mutants with functional defects in specific transport receptors. Thus, multiple functionally independent NPC translocation routes exist for different transport receptors. Our global analysis of the FG domain requirements in mRNA export also finds a requirement for two NPC substructures—one on the nuclear NPC face and one in the NPC central core. These results pinpoint distinct steps in the mRNA export mechanism that regulate NPC translocation efficiency.

Introduction

The nuclear envelope (NE) separates the contents of the nucleus and cytoplasm and is a physical barrier for the exchange of macromolecules. The only known mechanism for nuclear import and export is via nuclear pore complexes (NPCs; Fahrenkrog and Aebi, 2003; Fried and Kutay, 2003). Thus, the NPC is a central player in controlling gene expression and regulating nucleocytoplasmic signaling. Specifically, the NPC precludes molecules larger than ∼30–40 kD from freely diffusing through its central aqueous channel. Larger macromolecules use transport receptors to pass through the NPC in a signal-dependent process (Pemberton and Paschal, 2005). The karyopherin (Kap) β proteins (also termed importins, exportins, and/or transportins) are a major family of transport receptors. There are 14 Kapβs in budding yeast and >20 identified in higher eukaryotes (Harel and Forbes, 2004; Pemberton and Paschal, 2005). Each Kap binds a specific nuclear localization signal (NLS) or nuclear export sequence (NES) on a cargo, with Kap cargo release and transport directionality triggered by the small GTPase Ran (Fried and Kutay, 2003; Weis, 2003). There are non-Kapβ transport receptors for RanGDP import (Ntf2; Ribbeck et al., 1998; Smith et al., 1998) and for mRNA export (the heterodimer Mex67-Mtr2 [TAP/NXF1-p15/NXT1 in vertebrates]; Segref et al., 1997; Santos-Rosa et al., 1998; Katahira et al., 1999; Strasser et al., 2000). With the potential for at least 16 different receptors transporting thousands of distinct cargoes, the NPC is a complex machine. Indeed, it is not fully understood how such a myriad of distinct transport receptors use the NPC structure for presumably simultaneous translocation.

The ∼40–60-MD NPCs are formed by the assembly of multiple copies of ∼30 individual proteins called nucleoporins (Nups; Rout et al., 2000; Cronshaw et al., 2002). Nups associate in discrete subcomplexes and localize in specific substructures of the NPC, including the cytoplasmic filaments, the central core structure in the pore, and a nuclear basket structure (Fig. 1 B; Rout et al., 2000; Cronshaw et al., 2002; Fahrenkrog and Aebi, 2003). Movement of cargo-bound Kapβs, Ntf2, or Mex67-Mtr2 through the NPC requires interactions between the given transport receptor and a specialized subset of NPC proteins termed the FG (phenylalanine-glycine) Nups (Pemberton and Paschal, 2005). The FG Nups are defined by domains with numerous, clustered repeats of the core dipeptide FG flanked by characteristic spacer sequences (Rout and Wente, 1994). Nearly half of the Nups contain these FG domains, each with predominant FG subtypes (FG, FXFG [phenylalanine–any residue–phenylalanine-glycine], or

Correspondence to Susan R. Wente: susan.wente@vanderbilt.edu

Abbreviations used in this paper: cNLS, classic NLS; Kap, karyopherin; MBP, maltose-binding protein; mmp, more minimal pore; mRNP, messenger RNP; NE, nuclear envelope; NES, nuclear export sequence; NLS, nuclear localization signal; NPC, nuclear pore complex; Nup, nucleoporin; SC, synthetic complete.

The online version of this article contains supplemental material.

The Journal of Cell Biology, Vol. 178, No. 7, September 24, 2007 1121–1132
http://www.jcb.org/cgi/doi/10.1083/jcb.200704174

GLFG [glycine-leucine-phenylalanine-glycine]), defined NPC substructural locations, and corresponding orthologues across species (Rout et al., 2000; Cronshaw et al., 2002; Lim et al., 2006a). Some FG Nups are exclusively on the cytoplasmic (C) NPC fibrils (in *Saccharomyces cerevisiae* Nup159 and Nup42), and some are exclusively on the nuclear (N) NPC basket (in *S. cerevisiae* Nup1, Nup2, and Nup60); together, these are collectively defined as the asymmetric FG Nups (Fig. 1 B). The remaining FG Nups are distributed on both sides and through the central NPC channel and are termed the symmetric Nups (in *S. cerevisiae* Nup49, Nup57, Nsp1, Nup100, Nup116, and Nup145; Rout et al., 2000; Suntharalingam and Wente, 2003).

The physical interactions between transport receptors and FG peptides have been structurally analyzed for Kapβ1, Ntf2, and Nxt1. In these receptors, the Phe of an FG repeat is found in hydrophobic pockets on the protein surface (Bayliss et al., 2000a,b, 2002a,b; Fribourg et al., 2001). Indeed, transport receptor mutants with impaired FG binding are defective for NPC translocation (Bayliss et al., 2002b). Thus, each transport receptor serves as a molecular bridge between FG Nups and a signal-containing cargo. With multiple FG repeats per FG domain and multiple FG Nups in each NPC, the pore displays thousands of individual FG repeats, each of which is a potential binding site for a transport receptor. The abundance of FG repeats and sequence redundancies between FG Nups have made understanding the sequence of molecular interactions between the NPC and transport receptors a formidable task.

Given their critical role in the translocation mechanism, the FG Nups have been the focus of intense study. Models for the mechanism of NPC translocation have as their tenets the unfolded nature of the FG domains, the huge number of FG repeats per NPC, and the intrinsic binding affinities of transport receptors for FG domains. Localization of FG domains in the NPC and the physiological constraints of NPC translocation rates are also key considerations. Two of the fundamental models proposed contrast the FG domains as forming either a primarily physical or energetic barrier for selective translocation. As a physical barrier, weak interactions between FG domains are proposed to form a hydrophobic gel into which transport receptors selectively partition as a result of their FG interaction capacity (Ribbeck and Gorlich, 2002; Frey et al., 2006). The hydrophobic gel would form a selective phase and exclude macromolecules larger than the physical barrier generated by the FG interaction meshwork. As an energetic barrier, the interaction of a transport receptor with an FG Nup would allow the transport receptor to overcome an entropic threshold for diffusion through the NPC central channel (Rout et al., 2003). The FG domains would also function as repulsive bristles to entropically exclude nontransport receptor molecules (Lim et al., 2006b). As such, the NPC would be governed by a virtual gate. From the analysis of individual FG domains in vitro, there is independent data to support both the selective phase and virtual gate models.

To analyze the requirements for FG domains in the context of the intact NPC, we have used a large-scale genetic strategy in *S. cerevisiae* (Strawn et al., 2004). By combinatorial in-frame deletions in genes encoding the FG Nups, we showed that the asymmetric FG domains are dispensable for facilitated transport, whereas the symmetric FG domains are sufficient. Interestingly, although the selective-phase model predicts that the abundance or mass of FG repeats is critical to transport function (Macara, 2001; Ribbeck and Gorlich, 2001, 2002; Frey et al., 2006), we found that the number or mass of FG repeats does not correlate with in vivo transport capacity. We also found that for a given FG deletion (designated FGΔ) mutant, only a subset of the Kapβ transport receptors were perturbed. This suggests that different transport receptors require distinct combinations of FG domains for function (Strawn et al., 2004). In support of this, biochemical studies have demonstrated that different Kaps have different relative in vitro binding levels for the same FG Nup (Aitchison et al., 1996; Allen et al., 2001). There is also evidence that Kap95 might use different FG-binding sites than those used by Mex67 (Allen et al., 2001; Strawn et al., 2001; Blevins et al., 2003). Collectively, these studies suggest that the NPC may harbor multiple translocation pathways for different transport receptors.

To further investigate the FG-dependent transport pathways through the NPC, we generated a new collection of FG domain deletion mutants. We specifically compared Kapβ versus non-Kapβ translocation pathways by dissecting the requirements for Mex67-Mtr2–dependent mRNA export. Multiple laboratories have identified *nup*-null or temperature-sensitive alleles that cause mRNA export defects, and overproduction of the Nup116 GLFG domain inhibits mRNA export (Strasser and Hurt, 1999; Cole, 2000; Strawn et al., 2001). However, our new mutants have allowed the first global analysis of specific FG domain requirements in mRNA export. We have found striking differences in the requirements for Mex67-mediated mRNA export versus Kapβ-mediated transport. These results impact models for the in vivo NPC translocation mechanisms and support our hypothesis that multiple FG pathways exist for receptor-mediated translocation across the NPC.

Results

mmp FGΔ mutants have distinct Kap transport defects

In our previous study, we generated an *S. cerevisiae* mutant that lacked all of the asymmetric FG domains on the N and C faces of the NPC, which is designated the *ΔNΔC* mutant (Strawn et al., 2004). The *ΔNΔC* mutant has a slight rate delay in import via Kap95 and Kap104; however, it has no marked steady-state defect for any transport receptor assayed. Thus, the asymmetric FG domains do not serve essential functions. However, we speculated that the asymmetric FG domains could be key to maximal transport efficiency. In addition, because the FG domains can presumably occupy multiple topological positions in the NPC (Fahrenkrog et al., 2002; Denning et al., 2003; Lim et al., 2006b), it is possible that the asymmetric FG domains functionally compensate when individual symmetric FG domains are deleted. Therefore, we selected the *ΔNΔC* mutant as a foundation for studying the transport roles of individual symmetric FG domains. In frame, internal chromosomal deletions of the sequence encoding individual symmetric FG domains were constructed in the *ΔNΔC* background. If lethality was observed

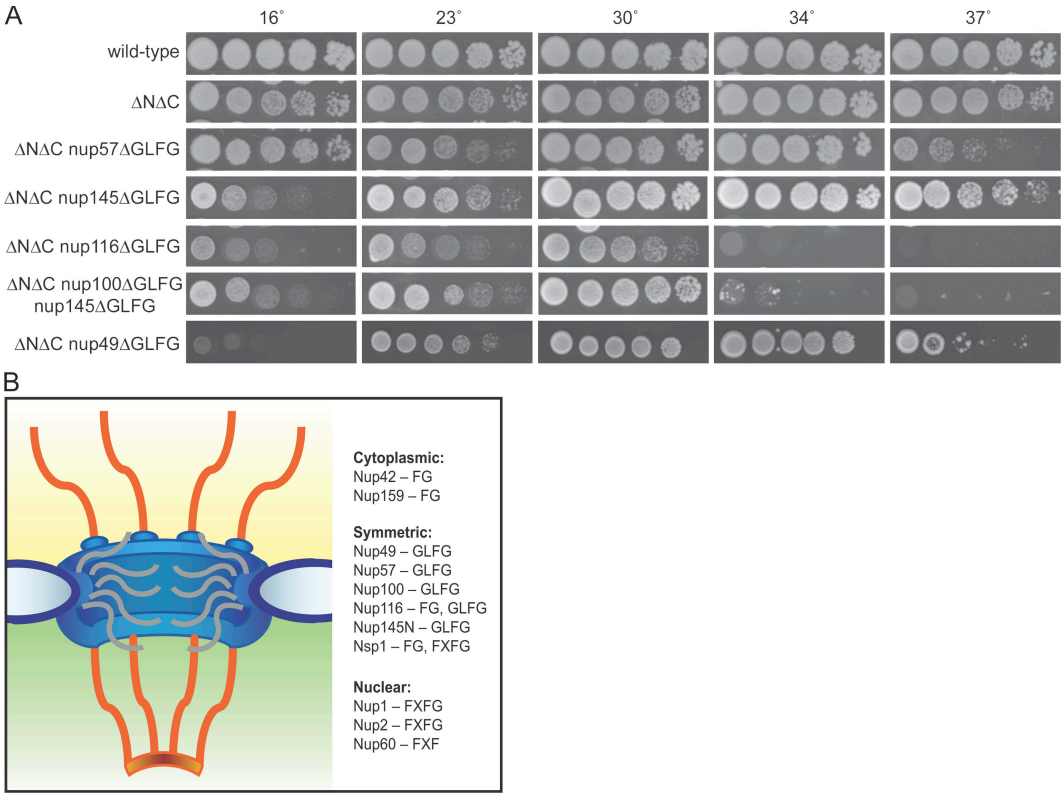

Figure 1. **The more minimal NPC (*mmp*) FGΔ mutants have temperature-sensitive growth defects.** (A) Wild-type, *ΔNΔC*, and new *mmp* FGΔ yeast strains were spotted onto YPD in fivefold serial dilutions and grown at the temperatures shown. (B) Schematic representation of the distribution of FG Nups within the NPC.

when a symmetric FG domain was removed in the *ΔNΔC* background, control complementation experiments were conducted with plasmids expressing the full-length *NUP* or FGΔ mutant versions (see Plasmids and yeast strains section in Materials and methods). This generated a series of *more minimal pore* (*mmp*) FGΔ mutant strains. Specifically, the *ΔNΔC* mutant was combined with individual deletions of the GLFG regions in Nup49, Nup57, Nup145, Nup100, Nup116, or the FG and FXFG regions in Nsp1. We found that all of the *mmp* FGΔ mutant strains with only one symmetric FG domain removed were viable (Fig. 1 A; Strawn et al., 2004). Additionally, the *ΔNΔC nup100ΔGLFG nup145ΔGLFG* mutant was viable despite having only four FG Nups intact (Nsp1, Nup49, Nup57, and Nup116).

The strains in this new *mmp* FGΔ mutant collection were characterized for growth properties at a range of temperatures. As shown in Fig. 1 A, the *ΔNΔC* mutant showed robust growth at all temperatures tested. In comparison, the *ΔNΔC nup57ΔGLFG* mutant had inhibited growth at 37°C, whereas the *ΔNΔC nup145ΔGLFG* mutant was cold sensitive at 16°C. The *ΔNΔC nup49ΔGLFG* mutant showed both temperature sensitivity at 37°C and cold sensitivity at 16°C. Overall, the *ΔNΔC nup116ΔGLFG* mutant and the *ΔNΔC nup100ΔGLFG nup145ΔGLFG* mutant strains had the most severe growth phenotypes with both temperature sensitivity at 34°C and cold sensitivity (Fig. 1 A). The *ΔNΔC nsp1ΔFGΔFXFG* mutant generated in our previous study is cold sensitive at 23°C and also inhibited at 37°C (Strawn et al., 2004).

We speculated that the temperature-dependent growth defects were linked to perturbations of an essential transport receptor. To test for defects in transport, the *mmp* FGΔ mutants were transformed with a panel of GFP-based reporters for different Kapβ transport receptors. Each transport reporter was based on a Kapβ- or Kapα-specific NLS fused to GFP or a tandem NLS-NES fused to GFP. In wild-type cells, all of the NLS-GFP reporters are predominantly nuclear, whereas NLS-NES-GFP is mostly cytoplasmic. The basic classic NLS (cNLS) of SV40 large T antigen is imported by the Kap95–Kap60 heterodimer (Shulga et al., 1996; Chook and Blobel, 2001), and Nab2 and the Nab2-NLS-GFP reporter are imported by Kap104 (Aitchison et al., 1996; Shulga et al., 2000). Spo12-NLS is recognized primarily by Kap121/Pse1 (Chaves and Blobel, 2001). The NLS-NES-GFP reporter includes a cNLS for Kap95–Kap60 import and a leucine-rich NES for Xpo1/Crm1 export (Stade et al., 1997). Steady-state transport assays in the wild-type and *mmp* FGΔ mutants were conducted at both the permissive temperature and after shifting to growth at 37°C for 1 h. The results are summarized in Table I. For all of the mutants, no defects at steady state were detected with either the cNLS (Kap95–Kap60) or NLS-NES-GFP (Crm1/Xpo1) reporters (Table I and not depicted). However, several of the mutants showed altered Spo12-NLS-GFP (Kap121) import. This included the *ΔNΔC* mutant combined with either the *nup100ΔGLFG*, *nsp1ΔFGΔFXFG*, *nup116ΔGLFG*, or *nup100ΔGLFG nup145ΔGLFG* alleles (Table I and Fig. 2; Strawn et al., 2004). At 37°C, the Spo12-NLS-GFP reporter

Table I. **Summary of transport assay results**

Strain	cNLS import	Nab2 import	Spo12NLS import	Leu-rich NES export	mRNA export
Wild type	+[a]	+[a]	+[a]	+[a]	+
nup100ΔGLFG nup145ΔGLFG nup57ΔGLFG	+[a]	−[a]	−[a]	+[a]	−
ΔNΔC	+[a]	+[a]	+/−[a]	+[a]	+
ΔNΔC nup57ΔGlFG	+	+	+	+	−
ΔNΔC nup100ΔGLFG	+[a]	+/−[a]	−[a]	+[a]	+
ΔNΔC nsp1ΔFGΔFXFG	+[a]	+/−[a]	−[a]	+[a]	+
ΔNΔC nup145ΔGLFG	+	+	+	+	+/−
ΔNΔC nup116ΔGLFG	+/−	−	−	+	+
ΔNΔC nup100ΔGLFG nup145ΔGlFG	+	+	−	+	+
ΔNΔC nup49ΔGlFG	+	+	+	+	−

Summary from the analysis of steady-state transport defects after shifting to growth at 37°C.
[a]Strawn et al., 2004.

showed a coincident increased cytoplasmic signal and decreased nuclear intensity in the *ΔNΔC nup100ΔGLFG nup145ΔGLFG* mutant and *ΔNΔC nup116ΔGLFG* mutant cells (Fig. 2 B). This indicated that these strains had defects in Kap121 transport.

Interestingly, only one of the *mmp* FGΔ mutant strains, *ΔNΔC nup116ΔGLFG*, showed a strong perturbation in steady-state Nab2 import by Kap104, with diminished nuclear localization and increased cytoplasmic signal at all growth temperatures. The defect was apparent using either the Nab2-NLS-GFP reporter (not depicted) or via indirect immunofluorescence for Nab2 localization (Fig. 2 A). Steady-state transport defects for Kap104 or Kap121 were not observed in the *ΔNΔC nup57ΔGLFG* mutant, the *ΔNΔC nup49ΔGLFG* mutant, or the *ΔNΔC nup145ΔGLFG* mutant strains (Fig. 2 and Table I). When comparing the Kap104 and Kap121 transport defects, it was especially striking that the *ΔNΔC nup100ΔGLFG nup145ΔGLFG* mutant showed differential perturbations. The Kap104 cargo Nab2 was efficiently imported (Fig. 2 A, far right), whereas the Kap121 reporter accumulated in the cytoplasm at 23 and 37°C (Fig. 2 B, far right). This is the first reported in vivo separation of FG-domain requirements for Kap104 and Kap121 NPC translocation. Overall, the *mmp* FGΔ mutant strains showed distinct defects for transport by specific Kaps.

Symmetric FGΔ and *mmp* FGΔ mutants have poly(A)$^+$ RNA export defects

To understand the contributions of FG domains to mRNA export, we screened a subset of our existing FGΔ mutant strains and our new *mmp* FGΔ mutant strains for mRNA export defects. This was evaluated using in situ hybridization with an oligo d(T) probe, which detects poly(A)$^+$ RNA. All of the viable FGΔ mutant strains with three symmetric FG domains deleted showed the nuclear accumulation of poly(A)$^+$ RNA after a 1-h shift to 37°C (Fig. 3, Table I, and not depicted). However, the *ΔNΔC* mutant cells did not show the nuclear accumulation of poly(A)$^+$ RNA. We also did not observe mRNA export defects in the *ΔNΔC nup100ΔGLFG* mutant, the *ΔNΔC nsp1ΔFGΔFXFG* mutant, the *ΔNΔC nup100ΔGLFG nup145ΔGLFG* mutant, or the *ΔNΔC nup116ΔGLFG* mutant cells. For mutants that showed no nuclear poly(A)$^+$ RNA accumulation, we also used an independent assay for mRNA export capacity and analyzed the effect on heat shock protein production. After heat shock in wild-type cells, elevated levels of Hsp104, Hsp82, Ssa4, and Ssa1 are a direct reflection of proper export and translation for the respective heat shock–induced mRNAs (Saavedra et al., 1997; Stutz et al., 1997). The *ΔNΔC* mutant and the *ΔNΔC nup116ΔGLFG* mutant were competent for heat shock protein production (unpublished data). We concluded that FG domains of the asymmetric FG Nups (Nup159, Nup42, Nup1, Nup2, and Nup60) and three specific symmetric FG Nups (Nup100, Nup116, and Nsp1) were not individually essential for mRNA export. In contrast, the *ΔNΔC nup57ΔGLFG* and the *ΔNΔC nup49ΔGLFG* mutant strains showed strong perturbations in mRNA export with marked nuclear accumulation of poly(A)$^+$ RNA (Fig. 3 and Table I). This indicated that Nup57 and/or Nup49 were preferentially required for mRNA export.

To further probe the requirements for the GLFG domains of Nup57 or Nup49, we examined a *nup57ΔGLFG nup49ΔGLFG* double mutant strain. The *nup57ΔGLFG nup49ΔGLFG* mutant was assayed for mRNA export defects. Nuclear poly(A)$^+$ RNA accumulation was observed in 9.9 ± 0.9% of the *nup57ΔGLFG nup49ΔGLFG* cells. Although this defect is significantly different from the level observed in wild-type cells ($P = 0.0031$), it is not as penetrant as the defect in either the *ΔNΔC nup49ΔGLFG* mutant or *ΔNΔC nup57ΔGLFG* mutant cells (30.3 ± 2.5% and 26.7 ± 6.1%, respectively). Thus, the GLFG domains of Nup57 and Nup49 are not essential for mRNA export, either individually or in combination. This suggested that other symmetric FG domains (Nup116, Nup100, Nup145, and Nsp1) functionally compensate in the absence of the Nup57 and Nup49 GLFG domains. However, when the asymmetric FG domains were removed (*ΔNΔC*), the GLFG domain of Nup57 or Nup49 was specifically required, and the FG domains from Nup116, Nup100, Nup145, and Nsp1 were not sufficient. Collectively, these results revealed a combinatorial requirement in mRNA export for specific GLFG domains with the asymmetric FG domains. Moreover, such differential requirements for FG domains in mRNA export were unanticipated. Previous studies have reported that Mex67 interacts in vitro with several of the asymmetric FG domains (Nup159, Nup42, Nup1, and Nup60) and with three symmetric FG domains (Nup100, Nup116, and Nsp1; Strasser et al., 2000; Allen et al., 2001; Strawn et al., 2001; Fischer et al., 2002).

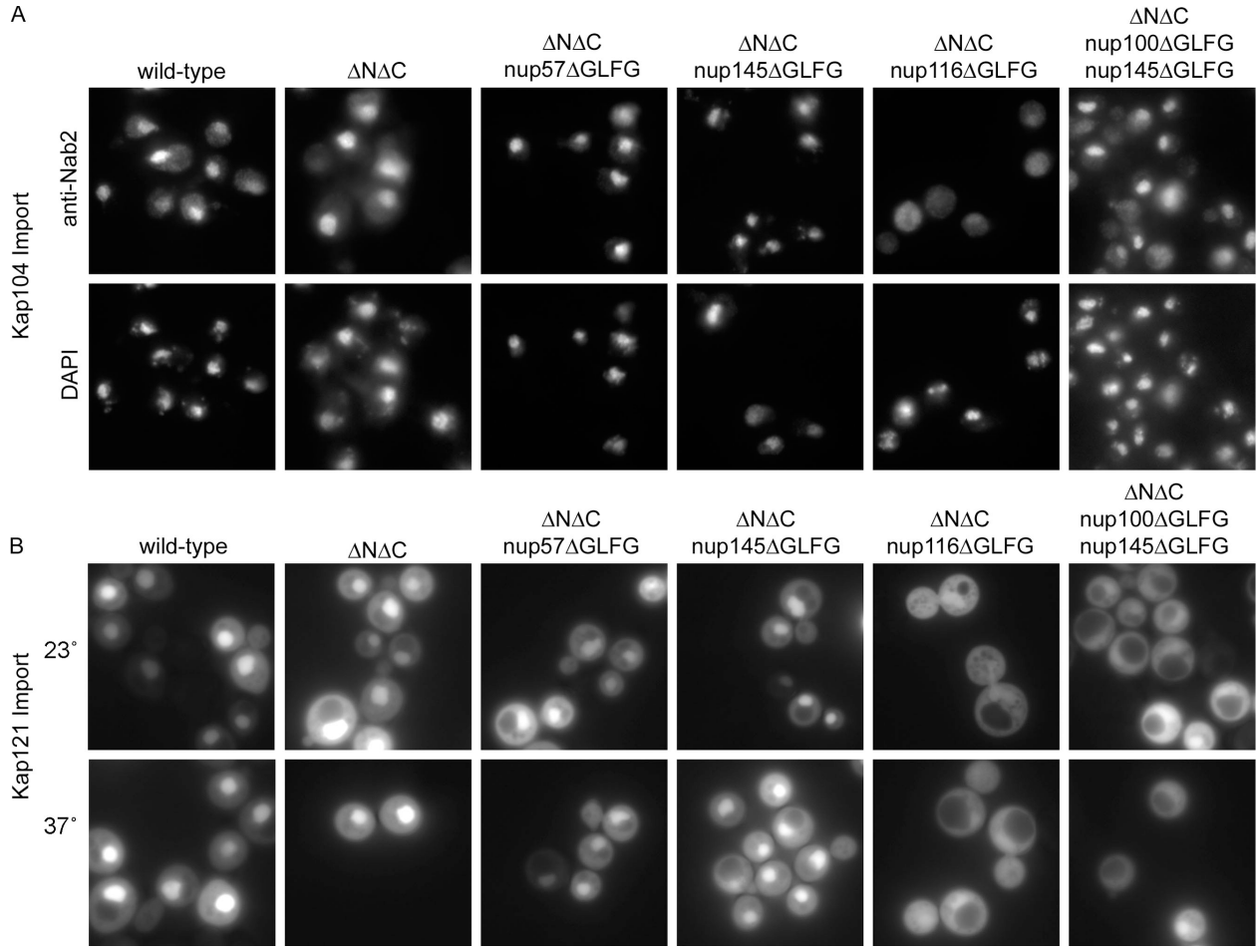

Figure 2. **The *mmp* FGΔ NPC mutants have distinct defects in Kap104 and Kap121 steady-state import.** (A) Indirect immunofluorescence with an anti-Nab2 antibody in yeast *mmp* FGΔ strains was conducted after a 1-h shift to 37°C. Nab2 localization, indicating Kap104 import, and DAPI-staining panels are shown. (B) Localization of a Spo12-NLS-GFP reporter, which is imported by Kap121, was evaluated at 23°C and after a 1-h shift to 37°C in *mmp* FGΔ strains.

Although the GLFG domains of Nup57 and Nup49 have not previously been reported to bind Mex67, these results suggested that the FG domains of Nup57 and Nup49 are key sites in vivo for mRNA export.

mRNA export requires GLFG domains of Nup57 and nuclear face Nups

Nup57 and Nup49 are both GLFG Nups that assemble in a heterotrimeric complex with Nsp1 (Grandi et al., 1993; Schlaich et al., 1997; Fahrenkrog et al., 1998). Given this shared NPC localization, the common FG types (GLFG), and the growth and transport phenotypes in the *mmp* FGΔ analysis, we concluded that the *ΔNΔC nup57ΔGLFG* mutant and *ΔNΔC nup49ΔGLFG* mutant strains were functionally comparable. We selected the *ΔNΔC nup57ΔGLFG* mutant for further analysis, as it was genotypically less complex (see Plasmids and yeast strains section in Materials and methods). To pinpoint which of the FG domains in the *ΔNΔC nup57ΔGLFG* mutant were most critical for mRNA export, we systematically generated strains with fewer FGΔ combinations. Each mutant strain was assayed for poly(A)$^+$ RNA localization by in situ hybridization with the oligo d(T) probe, and the percentage of cells in the population showing nuclear accumulation of poly(A)$^+$ RNA was scored (Fig. 4). The *nup57ΔGLFG* single mutant and the *ΔNΔC* mutant did not have defects, as the percentage of cells showing nuclear poly(A)$^+$ RNA accumulation was not significantly different from wild type ($P > 0.0602$). The *ΔC nup57ΔGLFG* mutant strain also did not have a poly(A)$^+$ RNA export defect. In contrast, *ΔN nup57ΔGLFG* mutant cells had a strong export defect after shifting to growth at 37°C for 1 h, with nearly 80% of the cells showing the nuclear accumulation of poly(A)$^+$ RNA. It was striking that the defect in the *ΔN nup57ΔGLFG* mutant (in 79.9 ± 9.4% of the cells at the assay time point) was more severe than that in the *ΔNΔC nup57ΔGLFG* mutant (in 26.7 ± 10.6% of the cells; see Discussion).

To further dissect the *ΔN nup57ΔGLFG* mutant phenotype, we assayed mutants with all possible FGΔ combinations of nuclear face FG domains (Nup1, Nup2, and Nup60) with the *nup57ΔGLFG* allele. The *nup1ΔFXFG nup2ΔFXFG nup57ΔGLFG* triple mutant had a poly(A)$^+$ RNA export defect with penetrance similar to the *ΔN nup57ΔGLFG* mutant (Fig. 4). This indicated that the *nup60ΔFXFG* allele did not contribute considerably to the *ΔN nup57ΔGLFG* mutant phenotype. In fact, addition of the *nup60ΔFXF* mutant allele to any single or

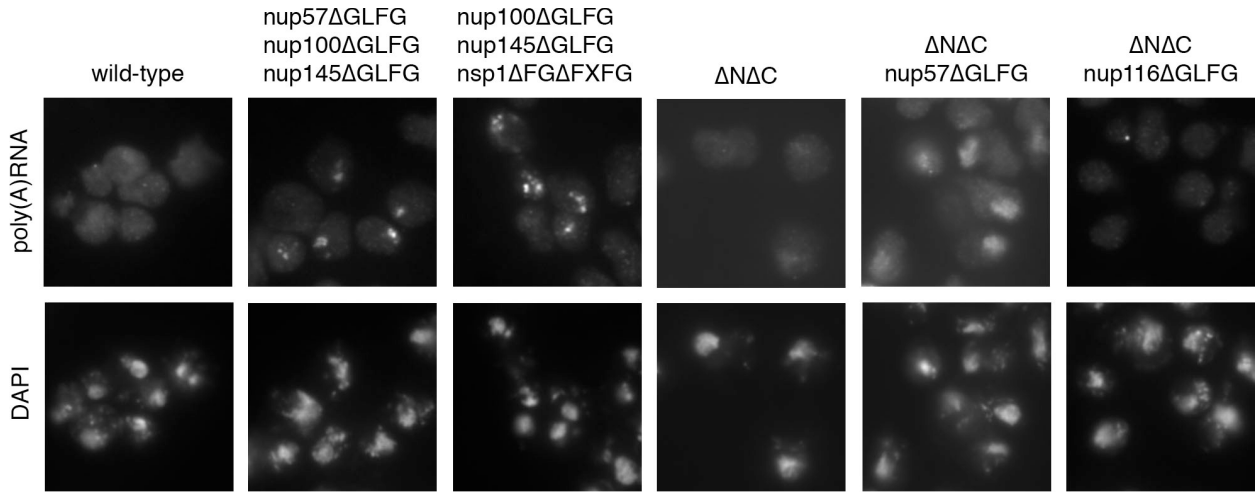

Figure 3. **mRNA export is inhibited in the symmetric *FGΔ* mutants and the *mmp* mutant *ΔNΔC nup57ΔGLFG*.** In situ hybridization with an oligo d(T) probe was conducted in the FGΔ NPC mutants after a 1-h shift to 37°C. Signal for the oligo d(T) probe indicates the subcellular distribution of poly(A)$^+$ RNA in comparison with the nuclear signal (by coincident DAPI staining).

double *FGΔ nup57ΔGLFG* mutant did not result in a statistically significant difference in the level of nuclear poly(A)$^+$ RNA accumulation ($P > 0.07$ for all comparisons). The *nup1ΔFXFG nup57ΔGLFG* double mutant and the *nup2ΔFXFG nup57ΔGLFG* double mutant strains also had defects; however, the percentage of cells with nuclear poly(A)$^+$ RNA accumulation was significantly less in the *nup1ΔFXFG nup57ΔGLFG* double mutant and *nup2ΔFXFG nup57ΔGLFG* double mutant strains than in the combined *nup1ΔFXFG nup2ΔFXFG nup57ΔGLFG* triple mutant ($P = 0.0018$ and $P = 0.0011$, respectively). Overall, these results suggested that the export of mRNA requires both a symmetric GLFG domain (Nup57 and Nup49) and the FXFG domains on the nuclear face (Nup1 and Nup2). This is the first evidence for an in vivo role for the specifically asymmetric FG domains in active NPC translocation.

Mex67 binds the Nup57 GLFG domain in vitro

We speculated that the deletion of FG domains critical for Mex67 docking at the NPC was the mechanistic basis for the mRNA export defects in the respective *mmp* FGΔ mutants. Specifically, the in vivo results suggested that Mex67 required binding sites in the FG domains of Nup57 or Nup49 and Nup1 or Nup2. Previous studies have documented that Mex67-Mtr2 can bind representative FG, FXFG, and GLFG domains (Strasser et al., 2000; Allen et al., 2001; Strawn et al., 2001). The FXFG domain of Nup1 has been directly analyzed (Strasser et al., 2000); however, tests of the Nup57 GLFG region have not been reported. We conducted studies to verify this interaction biochemically with recombinant proteins and a soluble binding assay. Clarified bacterial lysates from cells expressing GST alone or GST fused with the GLFG regions of Nup57 or Nup116 (GST-GLFG-Nup57 or GST-GLFG-Nup116) were incubated with glutathione-Sepharose. Purified maltose-binding protein (MBP)–Mex67 was then applied to the resin with the respective immobilized GST fusion proteins. As shown in Fig. 5, GST-GLFG-Nup57 bound MBP-Mex67, whereas GST alone did not bind MBP-Mex67. Binding was also detected between MBP-Mex67 and GST-GLFG-Nup116, as has previously been shown (Strawn et al., 2001). Thus, the GLFG domain of Nup57 directly binds Mex67 in vitro.

Efficient Mex67 recruitment to NPCs requires asymmetric FG domains and Nup57-GLFG

An mRNA export defect in an FGΔ mutant could result from either a direct effect on Mex67–NPC interactions or an indirect perturbation on Kap-mediated import of an essential mRNA export factor. We speculated that FGΔ mutants with primary defects in Mex67-mediated mRNA export would have decreased rates of Mex67-GFP recruitment to the NE/NPC as a result of the lack of critical FG-binding sites. To directly examine the dynamic properties of Mex67-GFP, we developed a live cell assay (Fig. 6 F). This strategy was based on the well-established assay for monitoring NLS-GFP import in live yeast cells (Shulga et al., 1996). Wild-type parental or FGΔ mutant cells expressing chromosomally tagged Mex67-GFP were incubated in glucose-free media in the presence of 10 mM 2-deoxy-D-glucose and 10 mM sodium azide for 45 min. This treatment results in cellular energy depletion and inhibits active nuclear transport (Shulga et al., 1996). The process of mRNA export is energy dependent (Paschal, 2002), at a minimum requiring the ATPase Dbp5 (Snay-Hodge et al., 1998; Tseng et al., 1998). As shown in Fig. 6, before energy depletion, all strains showed a strong Mex67-GFP signal at the nuclear rim. After energy depletion in all of the strains, Mex67-GFP was no longer concentrated at the NE/NPC, and the cytoplasmic and nuclear signals increased. Co-expression of a dsRed-HDEL (histidine-aspartate-glutamate-leucine; fusion protein with amino acid signal sequence for the ER retention) was used to facilitate visualization of the NE/ER. Localization of the dsRed-HDEL protein was not altered by energy depletion. As a control, we monitored the localization of two structural non-FG Nups, GFP-Nic96 and Nup170-GFP (Fig. 6 E), and found that a strong punctate NE/NPC signal was

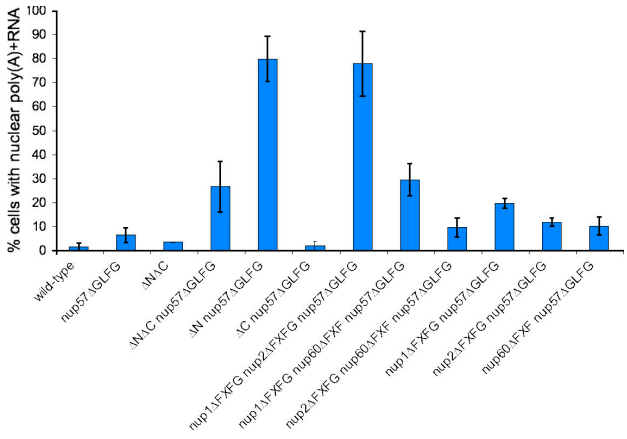

Figure 4. **mRNA export requires the FG domains of Nup57 and nuclear face Nups.** In situ hybridization with an oligo d(T) probe was conducted with the FGΔ strains indicated after a 1-h shift to 37°C. The percentage of cells showing the accumulation of poly(A)$^+$ RNA was calculated based on fields of >100 cells in three independent trials. Deletion of the nuclear face FG domains (*nup1ΔFXFG*, *nup2ΔFXFG*, and *nup60ΔFXF*) is abbreviated as ΔN. Deletion of the cytoplasmic face FG domains (*nup42ΔFG* and *nup159ΔFG*) is abbreviated as ΔC. Error bars represent SEM.

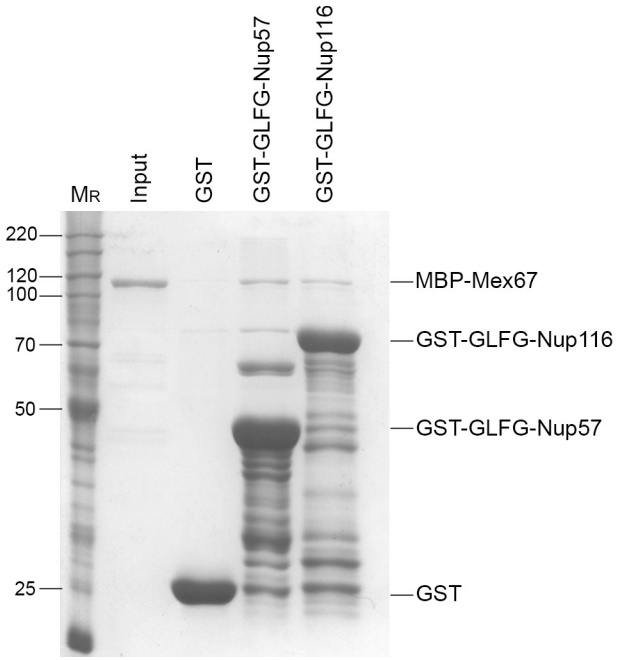

Figure 5. **Mex67 binds the GLFG domain of Nup57.** Bacterially expressed GST, GST-GLFG-NUP57, and GST-GLFG-NUP116 were each immobilized on glutathione agarose beads. Recombinant purified MBP-Mex67 was added, and the bound fraction was eluted. 10% of the input (MBP-Mex67) and the eluted fractions was resolved by SDS-PAGE and stained with Coomassie blue. Molecular mass (kilodaltons) markers are shown at the left (M_r).

present both before and after energy depletion. Nuclear rim localization of Nup49-GFP was also not altered by energy depletion in wild-type cells or in *ΔNΔC* mutant cells (Fig. 6 E and not depicted, respectively). This indicated that energy depletion results in the mislocalization of Mex67-GFP without a general perturbation of NE/NPC structure.

Using this assay, NE/NPC reassociation kinetics was determined by fluorescence microscopic monitoring of Mex67-GFP localization. At the start of the assay, the energy-depleted cells were washed and resuspended in 23°C glucose-containing media. The cells were then incubated until the NE/NPC signal recovered to pretreatment levels. Individual cells ($n > 150$) in a population were scored for normal continuous NE/NPC signal and relative levels of nucleoplasmic and cytoplasmic staining (Fig. 6 G). By plotting the percentage of cells with normal continuous NE/NPC signal as a function of time, relative association rates were determined. We then compared the association kinetics wherein a single variable was changed (e.g., the FGΔ mutant background).

After restoring energy to the system, Mex67-GFP in the wild-type cells returned to the pretreatment phenotype with Mex67-GFP predominantly at NE/NPCs (Fig. 6 A). The *ΔNΔC* mutant cells recovered more slowly than wild-type cells, and, at intermediate time points, an increased frequency of cells had elevated intranuclear signal relative to cytoplasmic. The recovery process in the *ΔNΔC nup57ΔGLFG* mutant was substantially more delayed. After 15 min, the *ΔNΔC nup57ΔGLFG* cells showed only a minimal recovery of Mex67-GFP localization to the NE/NPC. Moreover, at the intermediate time points, Mex67-GFP localization in the *ΔNΔC nup57ΔGLFG* cells was mostly intranuclear with no distinct NE/NPC staining (Fig. 6 C). This phenotype was also observed in the *ΔN nup57ΔGLFG* mutant, in which >50% of the cells accumulated Mex67-GFP in the nucleus and concentrated nuclear rim localization was not achieved over the time course of the assay (Fig. 6, D and G).

Again, as in the assays of poly(A)$^+$ RNA accumulation, the rate of Mex67-GFP localization to the NE/NPC was clearly more inhibited in the *ΔN nup57ΔGLFG* mutant than in the *ΔNΔC nup57ΔGLFG* mutant (see Discussion). Overall, we concluded that Mex67-GFP recruitment to the NPC in the *ΔNΔC nup57ΔGLFG* mutant and *ΔN nup57ΔGLFG* mutant was impaired. The intranuclear localization before distinct NE/NPC staining might reflect the efficient import of Mex67-GFP with specific mRNA export inhibition. These results correlate with our assays for poly(A)$^+$ RNA export and suggest that the *ΔNΔC nup57ΔGLFG* mutant and *ΔN nup57ΔGLFG* mutant are blocked for poly(A)$^+$ RNA export as a result of altered Mex67 recruitment to and/or translocation through the NPC.

Discussion

Many approaches have been used to study the mechanism by which transport receptors cross the NPC and the requirements for transport receptor interactions with FG Nups. We have used a genetic strategy in *S. cerevisiae* to generate extensive collections of mutants with specific combinations of FG domains removed and have conducted direct tests of the in vivo roles of putative FG-binding sites for transport receptors in the intact NPC (Strawn et al., 2004). In the present study, we report the analysis of new *mmp* FGΔ mutants wherein the symmetric FG domains were removed in the absence of all asymmetric FG domains (*ΔNΔC*). In some cases, the FGΔ phenotypes correlate directly with reported in vitro binding results. For example, previous studies have shown in vitro binding of Kap104 to the

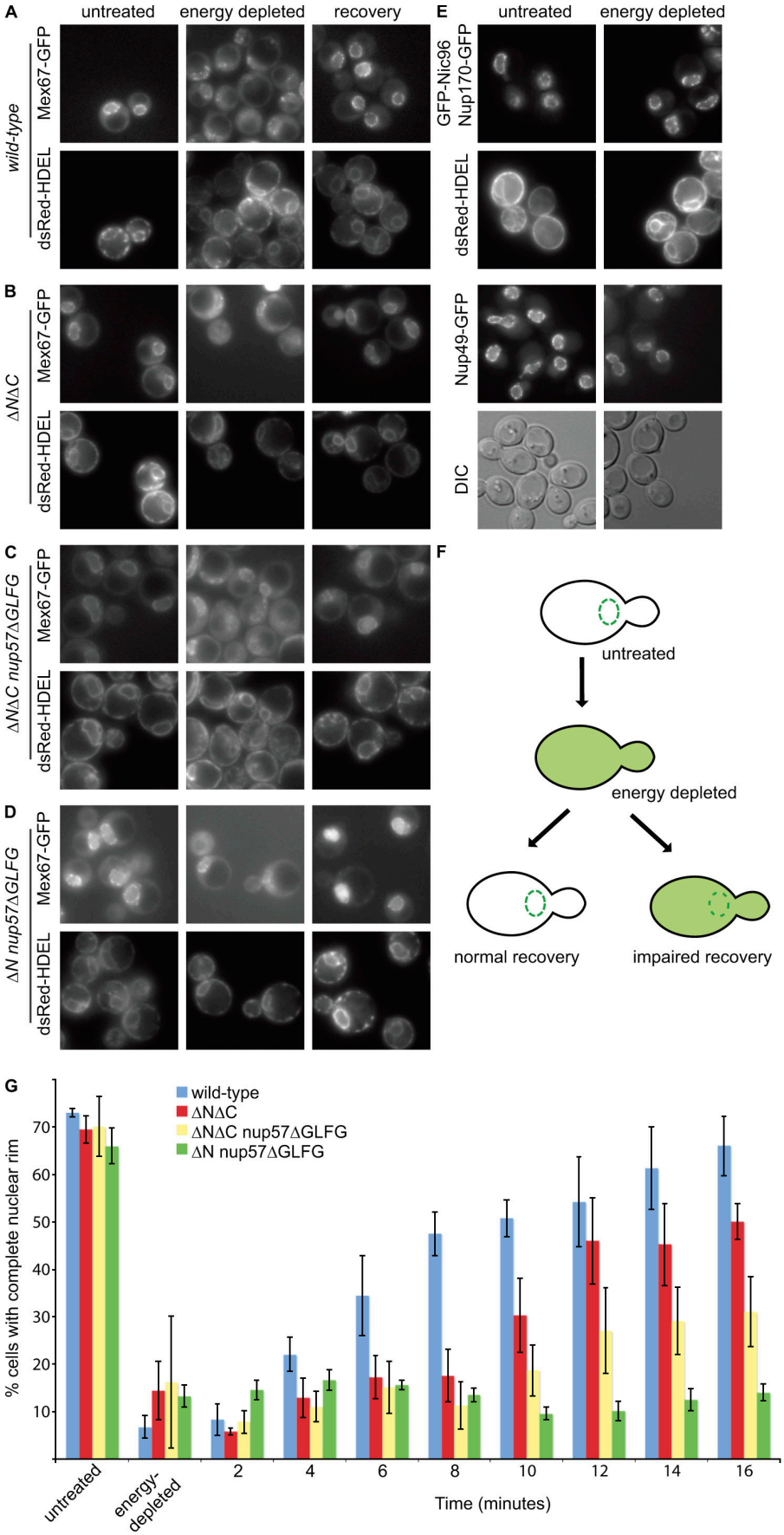

Figure 6. **Mex67-GFP recruitment to the NE/NPC is severely inhibited in both the *ΔNΔC nup57ΔGLFG* mutant and *ΔN nup57ΔGLFG* mutant.** (A–D) Mex67-GFP localization in representative wild-type (A), *ΔNΔC* (B), *ΔNΔC nup57ΔGLFG* (C), and *ΔN nup57ΔGLFG* (D) cells before the assay (untreated; left), after energy depletion (middle), or after 5-6 min of recovery from energy depletion (right). For each, the coincident localization of the ER marker dsRed-HDEL is shown. (E) As controls, the localization of GFP-Nic96 and Nup170-GFP or Nup49-GFP under the same conditions was evaluated. (F) A schematic diagram of the energy depletion assay for Mex67-GFP localization is shown. (G) The kinetics of Mex67-GFP recovery to the nuclear rim over time after energy depletion was determined. For three independent experiments, >150 cells were scored for the subcellular distribution of GFP signal at each time point. Error bars represent SEM. DIC, differential interference contrast.

Nup116 GLFG region (Aitchison et al., 1996; Allen et al., 2001), and, indeed, the *ΔNΔC nup116ΔGLFG* mutant has defects in Kap104-mediated transport, whereas the *ΔNΔC* mutant does not. This confirms that the Nup116 GLFG domain is a critical Kap104-binding site. On the other hand, we found that not all in vitro binding events are essential in vivo. Although Mex67 interacts with the GLFG region of Nup116 in vitro (Strasser et al., 2000; Strawn et al., 2001), the *ΔNΔC nup116ΔGLFG* mutant has no mRNA export defect. As a result, we conclude that in vitro binding between a transport receptor and an FG domain does not necessarily correlate with a requirement for that FG domain in vivo. Rather, the substructural location and physiological context of each FG domain is likely a key determinant in the organization of transport pathways through the NPC.

We have also identified binding events that were not previously recognized as important. We found that distinct combinations of both symmetric and asymmetric FG domains are needed for efficient nuclear export of poly(A)$^+$ RNA and recruitment of Mex67-GFP to the NE/NPC. This includes a GLFG domain from the symmetric Nup57 or Nup49 plus the asymmetric FXFG domains of Nup1 and Nup2 on the nuclear NPC face. Surprisingly, import by Kaps does not require these same FG domains. These results support a model wherein different transport receptors use distinct FG domains, allowing for multiple, preferred, and independent transport pathways through the NPC.

mRNA export requires the combinatorial use of distinct FG domains and non-FG–binding sites

Analysis of the *mmp* FGΔ mutants reveals that at least two FG-dependent steps are required for mRNA export through the NPC. We speculate that the locations in the NPC of the respective FG domains are key determinants for efficient mRNA export. The export cargo, a messenger RNP (mRNP) particle, is assembled cotranscriptionally and during mRNA processing (for review see Hieronymus and Silver, 2004). For such an mRNP, the first step in NPC translocation might require the nuclear face FXFG-binding sites in Nup1 and Nup2 for Mex67 recruitment to the NPC. In support of this hypothesis, the *ΔNΔC* mutant alone has a defect in the rate of Mex67-GFP recruitment to the NE/NPC. This also provides the first in vivo evidence that asymmetric FG domains contribute to the efficiency of mRNA export.

Second, after initial mRNP recruitment to the NPC, symmetrically localized FG domains are needed. Specifically, a GLFG domain from Nup57 or Nup49 in the symmetric Nsp1–Nup49–Nup57 subcomplex is required. Our results suggest that coupled interactions with the nuclear face FG domains and with Nup57 or Nup49 are required for mRNA export. Finally, after recruitment to the FXFG Nups on the nuclear face and translocation dependent on symmetric GLFG Nups, a third non-FG step in mRNA export is proposed at the cytoplasmic FG face. Interestingly, the asymmetric Nup159 and Nup42 FG domains on the cytoplasmic NPC face are not necessary for mRNA export when deleted on their own (*ΔC*; i.e., *nup159ΔFG nup42ΔFG*; unpublished data) or in combination with the *nup57ΔGLFG* mutant (the *ΔC nup57ΔGLFG* mutant). However, the flanking non-FG domains of Nup159 and Nup42 are required for mRNA export and serve as critical docking sites for the mRNA export factors Dbp5 and Gle1, respectively (Murphy and Wente, 1996; Hodge et al., 1999; Schmitt et al., 1999; Strahm et al., 1999; Weirich et al., 2004; Alcazar-Roman et al., 2006; Weirich et al., 2006).

It is striking that in two independent assays (poly(A)$^+$ RNA export and Mex67-GFP localization), the *ΔN nup57ΔGLFG* mutant had a more severe phenotype than the *ΔNΔC nup57ΔGLFG* mutant. In genetic terms, this indicates that the *ΔC* FG deletion partially suppressed the defect of the *ΔN nup57ΔGLFG* mutant. As such, the FG domains of Nup159 and Nup42 might play an inhibitory role during mRNA export in the intact NPC or a role in regulating terminal mRNP release. Mex67 is a potential target of the proposed Dbp5 RNP remodeling activity (Lund and Guthrie, 2005), and Mex67 binding to the respective Nup159 and Nup42 FG domains might influence this mechanism.

Overall, these results support a model with three coupled steps for the efficient and regulated export of mRNPs through the NPC. Alternatively, the mRNA export and Mex67-GFP recruitment defects in the *ΔNΔC nup57ΔGLFG* mutant and *ΔN nup57ΔGLFG* mutant strains could be caused by impaired mRNP assembly or disassembly rates. To date, however, only non-FG domains have been proposed as platforms for transport complex assembly or disassembly.

Nup49/Nup57 and Nup116 define two distinct pathways through the NPC

Our finding of unique transport defects in the *mmp* FGΔ mutants provides strong evidence for the existence of multiple independent transport pathways through the NPC. For example, the *ΔNΔC nup57ΔGLFG* mutant and *ΔNΔC nup49ΔGLFG* mutant strains have mRNA export defects but normal steady-state Kap104 import. In contrast, the *ΔNΔC nup116ΔGLFG* mutant has normal mRNA export but diminished steady-state Kap104 import. We propose that there are at least two distinct FG-dependent transport pathways through the NPC, which are defined by preferred FG-binding sites for different transport receptors. The data to date pinpoint the GLFG regions of Nup49/Nup57 and Nup116 as prime determinants for the different pathways. Interestingly, comparison of the five GLFG Nups indicates that single GLFG domains might be required differentially by transport receptors. There are several potential explanations for what defines such functional FG differences: (1) novel spacer sequences between FG repeats might contribute to the binding of transport receptors; (2) non-FG–binding sites adjacent to FG domains might be important, such as those defined for Kap95/Kap60 (Matsuura et al., 2003; Pyhtila and Rexach, 2003) and mRNA export components (Murphy and Wente, 1996; Murphy et al., 1996; Hodge et al., 1999; Schmitt et al., 1999; Strahm et al., 1999; Weirich et al., 2004); (3) the substructural location of the FG repeat domain (Lim et al., 2006a) and the conformations it can assume within the NPC (Fahrenkrog et al., 2002; Lim et al., 2006b); or (4) the number of repeats in the FG domain. Further dissection of the Nup49/Nup57 versus Nup116 GLFG domains should pinpoint the molecular basis for such functional differences.

These studies of the *mmp* FGΔ mutants also fully corroborate our previous conclusions from the analysis of asymmetric-specific versus symmetric-specific FGΔ mutants. We find no

correlation between the number of FG repeats deleted (or amount of FG mass removed) and the severity of transport defects. For example, the *ΔNΔC nup116ΔGLFG* mutant has 69.5% of its individual FG repeats remaining, yet it showed more severe transport defects than the *ΔNΔC nsp1ΔFGΔFXFG* mutant, which has only 47.5% of its individual FG repeats remaining (Strawn et al., 2004). Perhaps more importantly, even small-scale FG deletions have a dramatic impact on transport. For example, the *nup1ΔFXFG nup2ΔFXFG nup57ΔGLFG* mutant retains 84.9% of its FG repeats yet has a severe mRNA export defect, whereas the *ΔNΔC nup116ΔGLFG* mutant does not. Thus, there is no correlation between the number of FG repeats deleted and the level of mRNA export or Kap transport defects.

We predict that the substructural distribution and location of the critical FG-binding sites in the NPC is the fundamental basis for efficient transport. This conclusion is based on our findings of clear in vivo molecular requirements for distinct FG domains in different transport receptor mechanisms. Export of mRNA requires the GLFG domain of Nup57 or Nup49 in the Nic96–Nsp1–Nup49–Nup57 subcomplex. In contrast, Kap104 import requires the GLFG domain of Nup116 in the Nup82–Nsp1–Nup116 subcomplex. In regard to the debated models for NPC translocation (Ribbeck and Gorlich, 2002; Rout et al., 2003; Frey et al., 2006; Lim et al., 2006b), these results need to be taken into account. With distinct FG requirements, each transport receptor would have its own tailored set of FG-binding sites that form the basis of its given entropic barrier or selective phase for NPC entry and translocation. Overcoming an entropic or physical barrier of the NPC is thus achieved through binding to specific FG Nup domains.

A model of multiple NPC pathways allows for competition and regulation of transport

With multiple preferred FG-domain pathways, the transport of cargo by different receptors could be regulated by NPC structural changes and influenced by transport receptor relative abundance. *Aspergillus nidulans* undergoes partial NPC disassembly during mitosis, including the dissociation of several FG Nups from the NPC (De Souza et al., 2004; Osmani et al., 2006). These changes result in altered NPC permeability and transport and provide strong evidence that transport through the NPC can be regulated at the level of the NPC structure and FG Nup composition. Changes in NPC composition are also observed in virally infected cells, as interferon triggers up-regulation of the FG protein Nup98 as well as Nup96 and Rae1/Gle2 (Enninga et al., 2002). Influenza virus counteracts this antiviral response by forming an inhibitory complex with cellular mRNA export factors and by down-regulating Nup98. These mechanisms impair cellular mRNA export and favor viral mRNA export, which uses an alternative transport receptor (Neumann et al., 2000; Elton et al., 2001). Thus, the use of preferred FG-binding sites could allow unique mechanisms for the selective regulation of different transport pathways. Our collection of FGΔ mutants fully demonstrates the range and specificity of perturbations that could be accomplished by selective NPC composition changes.

Several studies have examined the effect of a given transport receptor's concentration on its own import efficiency (Riddick and Macara, 2005; Timney et al., 2006; Yang and Musser, 2006). Mathematical modeling has indicated that excess Kapβ/importinβ can impede its own translocation (Riddick and Macara, 2005), but experiments in permeabilized mammalian cells suggest that increased importinβ levels improve the efficiency of nuclear import (Yang and Musser, 2006). Recent experiments further show that modulating the levels of Kap123 in *S. cerevisiae* changes the import rate for Kap123 and its cargo in proportion to its abundance (Timney et al., 2006). However, exactly how the concentration of each Kapβ affects the transport of other molecules and receptors has not been examined. Given our proposal for independent FG-domain requirements by different transport receptors, in a wild-type NPC, direct competition for the same FG-binding sites or pathways might be prevented. However, if the FG Nup composition were to change, competition between receptors for the remaining pathways and FG-binding sites could impact translocation efficiency. Thus, either NPC structural changes at the level of individual FG domains (as shown here with the *FGΔ* mutants) or receptor competition could modulate nucleocytoplasmic trafficking and allow changes in nucleocytoplasmic transport flux in response to disease or developmental state. Further analysis of the transport properties in the FGΔ mutant collection will directly allow future tests of such regulated translocation models.

Materials and methods

Plasmids and yeast strains

Plasmids and yeast strains used in this study are listed in Tables S1 and S2 (available at http://www.jcb.org/cgi/content/full/jcb.200704174/DC1). Plasmid cloning was performed according to standard molecular biology strategies. Yeast strains were grown in YPD (1% yeast extract, 2% peptone, and 2% glucose) or in synthetic complete (SC) media with 2% glucose and lacking appropriate amino acids. New yeast FGΔ mutants were generated using a Cre-Lox system as previously described (Guldener et al., 1996; Strawn et al., 2004), with the exception of the *ΔNΔC nup49ΔGLFG* strain. Using the Cre-LoxP system, deletion of the sequence encoding amino acids 2–236 from *NUP49* was coincident with insertion of the sequence for a T7 epitope tag and a LoxP site fused in frame with the sequence encoding the C-terminal region of Nup49. The lethality of this *ΔNΔC nup49ΔGLFG*^{LoxP} strain was rescued by transformation with a *nup49ΔGLFG* plasmid (pSW3261). All assays were conducted with the *ΔNΔC nup49ΔGlFG*^{LoxP} *pSW3261* strain.

Microscopy and analysis of live cell GFP reporters

Yeast strains carrying pGAD-GFP (cNLS-GFP), pNS167 (Nab2NLS-GFP), pKW430 (NLS-NES-GFP$_2$), or pSpo12 $_{76–130}$-GFP (Spo12NLS-GFP) were grown to early log phase in SC media lacking the appropriate amino acid and supplemented with 2% glucose. Cells were examined from culture at 23°C or after 1-h shift to 37°C. All images were acquired using a microscope (BX50; Olympus) with a UPlanF1 100× NA 1.30 oil immersion objective (Olympus) and a camera (CoolSNAP HQ; Photometrics). Within each experiment, all images were collected and scaled identically. Images were collected using MetaVue version 4.6 (Molecular Devices) and processed with Photoshop 9.0 software (Adobe).

In situ hybridization and indirect immunofluorescence

Yeast cells were grown in YPD to early log phase at 23°C, and aliquots were shifted to 37°C for 1 or 3 h. Cells were fixed for 10 min and processed as previously described (Wente et al., 1992; Iovine et al., 1995). For indirect immunofluorescence, cells were incubated overnight with affinity-purified rabbit anti-Nab2 antibodies (1:4,000) and were detected with fluorescein-conjugated donkey anti–rabbit IgG (1:200; Jackson ImmunoResearch Laboratories). For in situ hybridization, cells were incubated overnight with a digoxigenin-dUTP–labeled oligo d(T) probe and were detected with fluorescein-labeled antidigoxigenin Fabs (1:25; Boehringer). DNA was stained with 0.1 μg/ml DAPI, and samples were mounted for

imaging in 90% glycerol and 1 mg/ml *p*-phenylenediamine (Sigma-Aldrich), pH 8.0. Images were acquired and processed as described in the previous section.

Protein purification and GST pull-down

GST, GST-GLFG-Nup57, and GST-GLFG-Nup116 were expressed in *Escherichia coli* Rosetta (DE3) cells (EMD Biosciences). Clarified lysates of GST fusion proteins were prepared in 20 mM Hepes, pH 7.5, 150 mM NaCl, and 20% wt/vol glycerol. MBP-Mex67 was expressed in Rosetta cells, affinity purified over amylose resin according to the manufacturer's protocol (New England Biolabs, Inc.), and dialyzed into binding buffer of 20 mM Hepes, pH 7.5, 150 mM NaCl, and 20% wt/vol glycerol. Clarified GST fusion protein lysates were bound to glutathione-Sepharose (GE Healthcare) and washed in binding buffer. MBP-Mex67 was applied to beads and incubated at 4°C for 30 min. Samples were washed twice in binding buffer and eluted on ice for 20 min in binding buffer, pH 7.5, with 20 mM glutathione. Equal fractions of bound protein were analyzed by SDS-PAGE and Coomassie blue staining.

Mex67-GFP NPC recruitment assay

MEX67 was chromosomally tagged with the sequence encoding GFP in haploid wild-type and FGΔ yeast by amplification of the *GFP:HIS3MX6* region from the yeast GFP collection strain YPL169C (Invitrogen). Integrants were selected on SC-histidine and verified by PCR and immunoblotting with rabbit anti-GFP (1:1,000). To allow integration of the gene for expression of dsRED-HDEL, YIplac204/TKC-DsRed-HDEL (Bevis et al., 2002) was linearized with EcoRV and transformed into yeast cells. Cells were selected on SC-tryptophan, and integrants were verified by live cell microscopy. For energy depletion assays, cells were grown to early log phase in YPD at 23°C. A culture aliquot of 2.5 A_{600} U was used, and the cells were pelleted, washed, and resuspended in 1 mL YP (without glucose) with 10 mM NaN_3 and 10 mM 2-deoxy-D-glucose. Cells were treated for 45 min at 23°C and were pelleted, washed, and placed on ice before microscopy. At time = 0, cells were resuspended in 23°C YPD, mounted on a glass slide, and visualized as described in Microscopy and analysis of live cell GFP reporters. Images of the GFP and dsRED signals were acquired every 30 s for 15 min. Cells were scored for the recovery of Mex67-GFP to the nuclear rim and the relative nuclear to cytoplasmic GFP signal. Control strains SWY734 and SWY3302 were examined before and immediately after energy depletion.

Online supplemental material

Table S1 lists the *S. cerevisiae* strains with genotypes and sources that are used in this study. Table S2 lists the plasmids used in this study and designates plasmid backbone and source. Online supplemental material is available at http://www.jcb.org/cgi/content/full/jcb.200704174/DC1.

Plasmids and yeast strains were provided by D. Goldfarb, G. Blobel, B. Glick, K. Weis, and J. Hegemann. We thank all members of the Wente laboratory for critical reading of the manuscript and discussion as well as past Wente laboratory members L. Strawn and D. Rexer for plasmid and strain construction.

This work was supported by a National Institutes of Health (NIH) grant (R01-GM51219) to S.R. Wente and a National Research Service Award NIH Virus, Nucleic Acids, and Cancer position (grant 5T32-CA009385) to L.J. Terry.

Submitted: 30 April 2007
Accepted: 21 August 2007

References

Aitchison, J.D., G. Blobel, and M.P. Rout. 1996. Kap104p: a karyopherin involved in the nuclear transport of messenger RNA binding proteins. *Science*. 274:624–627.

Alcazar-Roman, A.R., E.J. Tran, S. Guo, and S.R. Wente. 2006. Inositol hexakisphosphate and Gle1 regulate Dbp5 ATPase activity in mRNA export. *Nat. Cell Biol.* 8:711–716.

Allen, N.P., L. Huang, A. Burlingame, and M. Rexach. 2001. Proteomic analysis of nucleoporin interacting proteins. *J. Biol. Chem.* 276:29268–29274.

Bayliss, R., H.M. Kent, A.H. Corbett, and M. Stewart. 2000a. Crystallization and initial X-ray diffraction characterization of complexes of FxFG nucleoporin repeats with nuclear transport factors. *J. Struct. Biol.* 131:240–247.

Bayliss, R., T. Littlewood, and M. Stewart. 2000b. Structural basis for the interaction between FxFG nucleoporin repeats and importin-beta in nuclear trafficking. *Cell*. 102:99–108.

Bayliss, R., S.W. Leung, R.P. Baker, B.B. Quimby, A.H. Corbett, and M. Stewart. 2002a. Structural basis for the interaction between NTF2 and nucleoporin FxFG repeats. *EMBO J.* 21:2843–2853.

Bayliss, R., T. Littlewood, L.A. Strawn, S.R. Wente, and M. Stewart. 2002b. GLFG and FxFG nucleoporins bind to overlapping sites on importin-beta. *J. Biol. Chem.* 277:50597–50606.

Bevis, B.J., A.T. Hammond, C.A. Reinke, and B.S. Glick. 2002. De novo formation of transitional ER sites and Golgi structures in *Pichia pastoris*. *Nat. Cell Biol.* 4:750–756.

Blevins, M.B., A.M. Smith, E.M. Phillips, and M.A. Powers. 2003. Complex formation among the RNA export proteins Nup98, Rae1/Gle2 and TAP. *J. Biol. Chem.* 278:20979–20988.

Chaves, S.R., and G. Blobel. 2001. Nuclear import of Spo12p, a protein essential for meiosis. *J. Biol. Chem.* 276:17712–17717.

Chook, Y.M., and G. Blobel. 2001. Karyopherins and nuclear import. *Curr. Opin. Struct. Biol.* 11:703–715.

Cole, C.N. 2000. mRNA export: the long and winding road. *Nat. Cell Biol.* 2:E55–E58.

Cronshaw, J.M., A.N. Krutchinsky, W. Zhang, B.T. Chait, and M.J. Matunis. 2002. Proteomic analysis of the mammalian nuclear pore complex. *J. Cell Biol.* 158:915–927.

De Souza, C.P., A.H. Osmani, S.B. Hashmi, and S.A. Osmani. 2004. Partial nuclear pore complex disassembly during closed mitosis in *Aspergillus nidulans*. *Curr. Biol.* 14:1973–1984.

Denning, D.P., S.S. Patel, V. Uversky, A.L. Fink, and M. Rexach. 2003. Disorder in the nuclear pore complex: the FG repeat regions of nucleoporins are natively unfolded. *Proc. Natl. Acad. Sci. USA*. 100:2450–2455.

Elton, D., M. Simpson-Holley, K. Archer, L. Medcalf, R. Hallam, J. McCauley, and P. Digard. 2001. Interaction of the influenza virus nucleoprotein with the cellular CRM1-mediated nuclear export pathway. *J. Virol.* 75:408–419.

Enninga, J., D.E. Levy, G. Blobel, and B.M. Fontoura. 2002. Role of nucleoporin induction in releasing an mRNA nuclear export block. *Science*. 295:1523–1525.

Fahrenkrog, B., and U. Aebi. 2003. The nuclear pore complex: nucleocytoplasmic transport and beyond. *Nat. Rev. Mol. Cell Biol.* 4:757–766.

Fahrenkrog, B., E.C. Hurt, U. Aebi, and N. Pante. 1998. Molecular architecture of the yeast nuclear pore complex: localization of Nsp1p subcomplexes. *J. Cell Biol.* 143:577–588.

Fahrenkrog, B., B. Maco, A.M. Fager, J. Koser, U. Sauder, K.S. Ullman, and U. Aebi. 2002. Domain-specific antibodies reveal multiple-site topology of Nup153 within the nuclear pore complex. *J. Struct. Biol.* 140:254–267.

Fischer, T., K. Strasser, A. Racz, S. Rodriguez-Navarro, M. Oppizzi, P. Ihrig, J. Lechner, and E. Hurt. 2002. The mRNA export machinery requires the novel Sac3p-Thp1p complex to dock at the nucleoplasmic entrance of the nuclear pores. *EMBO J.* 21:5843–5852.

Frey, S., R.P. Richter, and D. Gorlich. 2006. FG-rich repeats of nuclear pore proteins form a three-dimensional meshwork with hydrogel-like properties. *Science*. 314:815–817.

Fribourg, S., I.C. Braun, E. Izaurralde, and E. Conti. 2001. Structural basis for the recognition of a nucleoporin FG repeat by the NTF2-like domain of the TAP/p15 mRNA nuclear export factor. *Mol. Cell*. 8:645–656.

Fried, H., and U. Kutay. 2003. Nucleocytoplasmic transport: taking an inventory. *Cell. Mol. Life Sci.* 60:1659–1688.

Grandi, P., V. Doye, and E.C. Hurt. 1993. Purification of NSP1 reveals complex formation with 'GLFG' nucleoporins and a novel nuclear pore protein NIC96. *EMBO J.* 12:3061–3071.

Guldener, U., S. Heck, T. Fielder, J. Beinhauer, and J.H. Hegemann. 1996. A new efficient gene disruption cassette for repeated use in budding yeast. *Nucleic Acids Res.* 24:2519–2524.

Harel, A., and D.J. Forbes. 2004. Importin beta: conducting a much larger cellular symphony. *Mol. Cell*. 16:319–330.

Hieronymus, H., and P.A. Silver. 2004. A systems view of mRNP biology. *Genes Dev.* 18:2845–2860.

Hodge, C.A., H.V. Colot, P. Stafford, and C.N. Cole. 1999. Rat8p/Dbp5p is a shuttling transport factor that interacts with Rat7p/Nup159p and Gle1p and suppresses the mRNA export defect of *xpo1-1* cells. *EMBO J.* 18:5778–5788.

Iovine, M.K., J.L. Watkins, and S.R. Wente. 1995. The GLFG repetitive region of the nucleoporin Nup116p interacts with Kap95p, an essential yeast nuclear import factor. *J. Cell Biol.* 131:1699–1713.

Katahira, J., K. Strasser, A. Podtelejnikov, M. Mann, J.U. Jung, and E. Hurt. 1999. The Mex67p-mediated nuclear mRNA export pathway is conserved from yeast to human. *EMBO J.* 18:2593–2609.

Lim, R.Y., U. Aebi, and D. Stoffler. 2006a. From the trap to the basket: getting to the bottom of the nuclear pore complex. *Chromosoma*. 115:15–26.

Lim, R.Y., N.P. Huang, J. Koser, J. Deng, K.H. Lau, K. Schwarz-Herion, B. Fahrenkrog, and U. Aebi. 2006b. Flexible phenylalanine-glycine nucleoporins as entropic barriers to nucleocytoplasmic transport. *Proc. Natl. Acad. Sci. USA*. 103:9512–9517.

Lund, M.K., and C. Guthrie. 2005. The DEAD-box protein Dbp5p is required to dissociate Mex67p from exported mRNPs at the nuclear rim. *Mol. Cell*. 20:645–651.

Macara, I.G. 2001. Transport into and out of the nucleus. *Microbiol. Mol. Biol. Rev.* 65:570–594.

Matsuura, Y., A. Lange, M.T. Harreman, A.H. Corbett, and M. Stewart. 2003. Structural basis for Nup2p function in cargo release and karyopherin recycling in nuclear import. *EMBO J.* 22:5358–5369.

Murphy, R., and S.R. Wente. 1996. An RNA-export mediator with an essential nuclear export signal. *Nature*. 383:357–360.

Murphy, R., J.L. Watkins, and S.R. Wente. 1996. GLE2, a *Saccharomyces cerevisiae* homologue of the *Schizosaccharomyces pombe* export factor RAE1, is required for nuclear pore complex structure and function. *Mol. Biol. Cell*. 7:1921–1937.

Neumann, G., M.T. Hughes, and Y. Kawaoka. 2000. Influenza A virus NS2 protein mediates vRNP nuclear export through NES-independent interaction with hCRM1. *EMBO J.* 19:6751–6758.

Osmani, A.H., J. Davies, H.L. Liu, A. Nile, and S.A. Osmani. 2006. Systematic deletion and mitotic localization of the nuclear pore complex proteins of *Aspergillus nidulans. Mol. Biol. Cell*. 17:4946–4961.

Paschal, B.M. 2002. Translocation through the nuclear pore complex. *Trends Biochem. Sci.* 27:593–596.

Pemberton, L.F., and B.M. Paschal. 2005. Mechanisms of receptor-mediated nuclear import and nuclear export. *Traffic*. 6:187–198.

Pyhtila, B., and M. Rexach. 2003. A gradient of affinity for the karyopherin Kap95p along the yeast nuclear pore complex. *J. Biol. Chem.* 278:42699–42709.

Ribbeck, K., and D. Gorlich. 2001. Kinetic analysis of translocation through nuclear pore complexes. *EMBO J.* 20:1320–1330.

Ribbeck, K., and D. Gorlich. 2002. The permeability barrier of nuclear pore complexes appears to operate via hydrophobic exclusion. *EMBO J.* 21:2664–2671.

Ribbeck, K., G. Lipowsky, H.M. Kent, M. Stewart, and D. Gorlich. 1998. NTF2 mediates nuclear import of Ran. *EMBO J.* 17:6587–6598.

Riddick, G., and I.G. Macara. 2005. A systems analysis of importin-α-β mediated nuclear protein import. *J. Cell Biol.* 168:1027–1038.

Rout, M.P., and S.R. Wente. 1994. Pores for thought: nuclear pore complex proteins. *Trends Cell Biol.* 4:357–365.

Rout, M.P., J.D. Aitchison, A. Suprapto, K. Hjertaas, Y. Zhao, and B.T. Chait. 2000. The yeast nuclear pore complex: composition, architecture, and transport mechanism. *J. Cell Biol.* 148:635–651.

Rout, M.P., J.D. Aitchison, M.O. Magnasco, and B.T. Chait. 2003. Virtual gating and nuclear transport: the hole picture. *Trends Cell Biol.* 13:622–628.

Saavedra, C.A., C.M. Hammell, C.V. Heath, and C.N. Cole. 1997. Yeast heat shock mRNAs are exported through a distinct pathway defined by Rip1p. *Genes Dev.* 11:2845–2856.

Santos-Rosa, H., H. Moreno, G. Simos, A. Segref, B. Fahrenkrog, N. Pante, and E. Hurt. 1998. Nuclear mRNA export requires complex formation between Mex67p and Mtr2p at the nuclear pores. *Mol. Cell. Biol.* 18:6826–6838.

Schlaich, N.L., M. Haner, A. Lustig, U. Aebi, and E.C. Hurt. 1997. In vitro reconstitution of a heterotrimeric nucleoporin complex consisting of recombinant Nsp1p, Nup49p, and Nup57p. *Mol. Biol. Cell*. 8:33–46.

Schmitt, C., C. von Kobbe, A. Bachi, N. Pante, J.P. Rodrigues, C. Boscheron, G. Rigaut, M. Wilm, B. Seraphin, M. Carmo-Fonseca, and E. Izaurralde. 1999. Dbp5, a DEAD-box protein required for mRNA export, is recruited to the cytoplasmic fibrils of nuclear pore complex via a conserved interaction with CAN/Nup159p. *EMBO J.* 18:4332–4347.

Segref, A., K. Sharma, V. Doye, A. Hellwig, J. Huber, R. Luhrmann, and E. Hurt. 1997. Mex67p, a novel factor for nuclear mRNA export, binds to both poly(A)$^+$ RNA and nuclear pores. *EMBO J.* 16:3256–3271.

Shulga, N., P. Roberts, Z. Gu, L. Spitz, M.M. Tabb, M. Nomura, and D.S. Goldfarb. 1996. *In vivo* nuclear transport kinetics in *Saccharomyces cerevisiae*: a role for heat shock protein 70 during targeting and translocation. *J. Cell Biol.* 135:329–339.

Shulga, N., N. Mosammaparast, R. Wozniak, and D.S. Goldfarb. 2000. Yeast nucleoporins involved in passive nuclear envelope permeability. *J. Cell Biol.* 149:1027–1038.

Smith, A., A. Brownawell, and I.G. Macara. 1998. Nuclear import of Ran is mediated by the transport factor NTF2. *Curr. Biol.* 8:1403–1406.

Snay-Hodge, C.A., H.V. Colot, A.L. Goldstein, and C.N. Cole. 1998. Dbp5p/Rat8p is a yeast nuclear pore-associated DEAD-box protein essential for RNA export. *EMBO J.* 17:2663–2676.

Stade, K., C.S. Ford, C. Guthrie, and K. Weis. 1997. Exportin 1 (Crm1p) is an essential nuclear export factor. *Cell*. 90:1041–1050.

Strahm, Y., B. Fahrenkrog, D. Zenklusen, E. Rychner, J. Kantor, M. Rosbach, and F. Stutz. 1999. The RNA export factor Gle1p is located on the cytoplasmic fibrils of the NPC and physically interacts with the FG-nucleoporin Rip1p, the DEAD-box protein Rat8p/Dbp5p and a new protein Ymr 255p. *EMBO J.* 18:5761–5777.

Strasser, K., and E. Hurt. 1999. Nuclear RNA export in yeast. *FEBS Lett.* 452:77–81.

Strasser, K., J. Bassler, and E. Hurt. 2000. Binding of the Mex67p/Mtr2p heterodimer to FXFG, GLFG, and FG repeat nucleoporins is essential for nuclear mRNA export. *J. Cell Biol.* 150:695–706.

Strawn, L.A., T. Shen, and S.R. Wente. 2001. The GLFG regions of Nup116p and Nup100p serve as binding sites for both Kap95p and Mex67p at the nuclear pore complex. *J. Biol. Chem.* 276:6445–6452.

Strawn, L.A., T. Shen, N. Shulga, D.S. Goldfarb, and S.R. Wente. 2004. Minimal nuclear pore complexes define FG repeat domains essential for transport. *Nat. Cell Biol.* 6:197–206.

Stutz, F., J. Kantor, D. Zhang, T. McCarthy, M. Neville, and M. Rosbash. 1997. The yeast nucleoporin Rip1p contributes to multiple export pathways with no essential role for its FG-repeat region. *Genes Dev.* 11:2857–2868.

Suntharalingam, M., and S.R. Wente. 2003. Peering through the pore. Nuclear pore complex structure, assembly, and function. *Dev. Cell*. 4:775–789.

Timney, B.L., J. Tetenbaum-Novatt, D.S. Agate, R. Williams, W. Zhang, B.T. Chait, and M.P. Rout. 2006. Simple kinetic relationships and nonspecific competition govern nuclear import rates in vivo. *J. Cell Biol.* 175:579–593.

Tseng, S.S., P.L. Weaver, Y. Liu, M. Hitomi, A.M. Tartakoff, and T.H. Chang. 1998. Dbp5p, a cytosolic RNA helicase, is required for poly(A)$^+$ RNA export. *EMBO J.* 17:2651–2662.

Weirich, C.S., J.P. Erzberger, J.M. Berger, and K. Weis. 2004. The N-terminal domain of Nup159 forms a beta-propeller that functions in mRNA export by tethering the helicase Dbp5 to the nuclear pore. *Mol. Cell*. 16:749–760.

Weirich, C.S., J.P. Erzberger, J.S. Flick, J.M. Berger, J. Thorner, and K. Weis. 2006. Activation of the DExD/H-box protein Dbp5 by the nuclear-pore protein Gle1 and its coactivator InsP6 is required for mRNA export. *Nat. Cell Biol.* 8:668–676.

Weis, K. 2003. Regulating access to the genome. Nucleocytoplasmic transport throughout the cell cycle. *Cell*. 112:441–451.

Wente, S.R., M.P. Rout, and G. Blobel. 1992. A new family of yeast nuclear pore complex proteins. *J. Cell Biol.* 119:705–723.

Yang, W., and S.M. Musser. 2006. Nuclear import time and transport efficiency depend on importin β concentration. *J. Cell Biol.* 174:951–961.